



Supplementary Information for

Catastrophic ATP loss underlies a metabolic combination therapy tailored for MYCN-amplified neuroblastoma

Krista M. Dalton^{a,*}, Timothy L. Lochmann^{a,*}, Konstantinos V. Floros^a, Marissa L. Calbert^a, Richard Kurupi^a, Giovanna T. Stein^{b, c}, Joseph McClanaghan^{b, c}, Ellen Murchie^{b, c}, Regina K. Egan^{b, c}, Patricia Greninger^{b, c}, Mikhail Dozmorov^d, Sivapriya Ramamoorthy^e, Madhavi Puchalapallif, Bin Huf, Lisa Shock^g, Jennifer Koblinski^f, John Glod^h, Sosipatros A. Boikosⁱ, Cyril H. Benes^{b, c, ^}, and Anthony C. Faber^{a, ^}

^aPhilips Institute for Oral Health Research, VCU School of Dentistry and Massey Cancer Center, Virginia Commonwealth University, Richmond, VA 23298; ^bCenter for Cancer Research, Massachusetts General Hospital Cancer Center, Boston, MA 02129; ^cDepartment of Medicine, Harvard Medical School, Boston, MA 02115; ^dDepartment of Biostatistics, Virginia Commonwealth University, Richmond, VA 23298; ^eDiscovery and Translational Sciences, Metabolon, Inc., Research Triangle Park, NC 27709; ^fDepartment of Pathology, Virginia Commonwealth University, Richmond VA, 23298; ^gDepartment of Microbiology and Immunology, Virginia Commonwealth University, Richmond VA, 23298; ^hPediatric Oncology Branch, National Cancer Institute, National Institutes of Health, Bethesda, MD 20892; ⁱDepartment of Internal Medicine, Virginia Commonwealth University, Richmond, VA, 23298

[^]co-corresponding authors: Cyril H. Benes, Anthony C. Faber
Email: cyrilbenes@gmail.com, acfaber@vcu.edu

This PDF file includes:

- Materials and Methods
- Supplemental References
- Figures S1 to S10
- Table S1
- Legends for Datasets S1 to S5

Materials and Methods

Expression analysis. RNA-seq data from a recent study (5) (GEO accession no. GSE80153) was used to analyze the expression of mitochondrial genes using the DAVID tool as previously described (39) (Fig. 4A). The expression of MCT4 for multiple cancer cell lines was determined from the CCLE (Fig. 5B). Patient data and gene expression datasets were obtained from the R2:Genomics analysis and visualization platform. All analyses were performed with R2 and all data and *P*-values were downloaded. Kaplan-Meier analysis was performed, and the resulting survival curves were generated. All cutoff values for generating high and low expression groups were determined using the online R2 database algorithm. ChIP-seq data from a recent study (55) were used to examine MYCN binding throughout the genome in neuroblastomas (Fig. 8 D and E).

Drug screening and genomic modeling. Authenticated cell lines from the GDSC were screened against phenformin and AZD3965 (Fig. 1A). RNA expression data for sarcoma samples (Fig. 1A) were obtained and analyzed through the R2: Genomic Analysis and Visualization Platform (<https://hgserver1.amc.nl/cgi-bin/r2/main.cgi>). HTS was performed using variable concentration of single agents across 9 doses using 2-fold serial dilutions (256 fold range). Phenformin was screened at a maximum dose of 2 mM, and AZD3965 was screened at a maximum dose of 256 nM. Combinations of either AZD3965 at a fixed dose of 128nM added to a variable dose of phenformin (Max dose 2 mM) or phenformin at a fixed dose of 125 μ M combined to a variable dose of AZD3569 (256 nM max dose) were also screened. Drugs were added to cells for 5 d. Cellular viability was determined using resazurin and the area under the dose-response curve was determined using the drexplorer R package (Ref doi: 10.1093/bioinformatics/btv028) and used throughout the analyses as the sensitivity metric. A Kolmogorov-Smirnov (KS) two sample test was used to determine statistical significance of the differential sensitivity of *MYCN*-amplified cell lines compared to *MYCN* wild-type cell lines to drug treatments. Elastic net regression modeling of the AUC data using genomics data available for the cell lines (42) was performed as previously described (24). In the model output (Dataset S5), gene expression features associated with a positive effect value correspond to genes with higher expression in more resistant cell lines (high AUC values associated with high gene expression values).

Western blotting. Cells were lysed with lysis buffer (20mM Tris, 150mM NaCl, 1% NP-40, 1 mM EDTA, 1mM EGTA, 10% glycerol, and protease and phosphatase inhibitors), incubated on ice for 10 min and centrifuged at 10,500 rpm for 10 min at 4 °C. Equal amounts of the detergent-soluble lysates were resolved using the NuPAGE® Novex® Midi Gel system on 4% to 12% Bis-Tris Gels (Invitrogen), transferred to polyvinylidene difluoride membranes (PerkinElmer) in between 6 pieces of Whatman paper (Fisher Scientific), set in transfer buffer from Biorad with 20% methanol, and following transfer and blocking in 5% non-fat milk in phosphate buffered saline, probed overnight with the antibodies listed below. Chemiluminescence was detected with the Syngene G:Box camera (Synoptics). Antibodies used at a dilution of 1:1000 in 5% bovine serum albumin-tris-buffered saline with Tween 20 are as follows: from Cell Signaling Technologies cleaved PARP (catalog #5625), phospho-mTOR (Ser2481) (catalog #2974), phospho-AMPK (Thr172) (catalog #50081), phospho-S6 ribosomal protein (Ser240/244) (catalog #2215), ATF4 (catalog #11815), IRE1- α (catalog #3294), β -actin (catalog #4970), and from SantaCruz Biotechnology MYCN (sc-53993), MCT1 (sc-365501), and MCT4 (sc-376140).

Cell viability. Neuroblastoma cells were seeded in quadruplicate in 96 well microtiter plates at a concentration of 2×10^3 cells per well in 180 μ l of growth medium and after 24 h, cells were

treated with drug for either 16 h (Fig. 6F, and *SI Appendix*, Figs. S3, S6, and S7) or 72 h (Fig. 2 and Fig. 9A). Cell viability was measured by the CellTiter-Glo protocol per the manufacturer (Promega). Drug synergy was determined using the Bliss independence model and is defined as the difference between the calculated inhibition value if the two agents act independently and the observed combined inhibition values. Positive Bliss scores represent dose combinations in which the effect is greater than additive.

Crystal violet. Cells were seeded at 5×10^4 cells per well in a six well dish and treated the following day with AZD3965, phenformin, or the combination of both. Five or six days later, when untreated cells reached confluency, cells were stained with 0.1% crystal violet (Sigma-Aldrich).

Xenograft and patient-derived xenograft models. The COG-N-561 PDX model from the Children's Oncology Group (COG) Cell Culture and Xenograft Repository and the SMS-SAN *MYCN*-amplified model were injected into female NOD-*scid*-IL2R γ ^{null} mice (purchased from VCU Cancer Mouse Models Core Laboratory) at 2×10^6 cells per flank on both flanks of the mouse using a 1:1 ratio of cells/Matrigel (Corning, catalog#354248). The SMS-SAN injected mice were randomized when they reached an average tumor size of 145 mm³, with cohorts being three mice per treatment. The COG-N-561 injected mice were randomized once tumors reached an average tumor size of 200 mm³, with cohorts consisting of three controls, three phenformin treated, four AZD3965 treated, and four combination treated. The mice were randomized using the 2 factor (tumor volume and body weight) randomization Multi-Task tool in Studylog lab management software. The mice were treated with AZD3965 (100 mg/kg/qd/po) and phenformin (100 mg/kg/qd/po) by oral gavage (100 μ L; 0.5% hydroxypropylmethylcellulose, 0.1% tween 80, and 0.49% water) 5 d/wk for 2 wk. For the blood toxicity study, NSG mice were treated with no drug, AZD3965, phenformin, or the combination, at the same doses as above. At 3 d mice were exsanguinated, and blood was sent to IDEXX BioResearch for testing. The recovery cohort was treated for 7 d and allowed 24 h of recovery from treatment before exsanguination. All animal experiments were approved by the Virginia Commonwealth University (VCU) Institutional Animal Care and Use Committee (protocol #AD10001048).

Seahorse respiratory experiments. Before seeding, XF microplates were coated with 20 μ l of 50 μ g/ml of poly-D-lysine. After 1 h the poly-D-lysine was aspirated off and the wells were washed with deionized water. The IMR5 cells were seeded at a concentration of 2×10^3 in 180 μ l of XF media, with 4 wells with only XF media for background correction and incubated overnight. Cells were treated with drug for 16 h (Fig. 3 A and B) and loaded into an Agilent Seahorse XFp analyzer with a sensor cartridge that had been incubated in 200 μ l of calibrant overnight, or cells were not treated with drug and loaded into the analyzer with the sensor cartridge port A containing AZD3965 and port B containing phenformin (Fig. 3 D and E), and baseline OCR and ECAR was measured. The RPE.1 GFP and RPE.1 *MYCN* cells were seeded same as described above and loaded into the analyzer with sensor cartridge port A containing 20 μ l oligomycin, port B containing 22 μ l FCCP, and port C containing 24 μ l rotenone + antimycin A for the mitochondrial stress test.

Lentivirus production. The pMXs-hu-N-Myc plasmid was a gift from Shinya Yamanaka (University of California, San Francisco; Addgene plasmid # 50772; www.addgene.org/50772/; RRID: Addgene_50772) and has been previously described (70). It was cloned into the pLenti backbone to form pLENTI-MYCN. The MCT4 plasmid was obtained from OriGene (cat# RC211987L3), cloned into the pLenti backbone, and lentiviral production was performed as previously described (71).

siRNA. The *ATF4* siRNA (cat. #L005125-00-0005) and scramble (siSCR) control siRNA (cat. #D-001810-10-20) were purchased from Dharmacon. The *MYCN* siRNA (cat. #SI03087518) was purchased from Qiagen, and the *MCT1* siRNA (sc-37235) was purchased from Santa Cruz Biotechnologies. Lipofectamine RNAiMAX Transfection Reagent (ThermoFisher Scientific) was used to produce the knockdown cells with 50 nmol/L of siRNAs, following the manufacturer's protocol.

ATP/ADP. The RPE.1, CHLA20, and CHLA172 GFP and MYCN expressing cells were treated with 1 μ M AZD3965, 10 μ M phenformin, or the combination of both for 16 h and ATP/ADP ratio was measured by ADP/ATP Ratio Assay Kit protocol per the manufacturer (abcam) protocol, where ATP/ADP ratio was calculated by $1 - [\text{Data D} - \text{Data C}] / [\text{Data B} - \text{Data A}]$.

Glucose Uptake. The IMR5 and SK-N-BE(2) cells were treated with 1 μ M AZD3965, 10 μ M phenformin, or the combination of both for 16 h, and the glucose uptake was measured by the Glucose Uptake-Glo Assay protocol per the manufacturer (Promega).

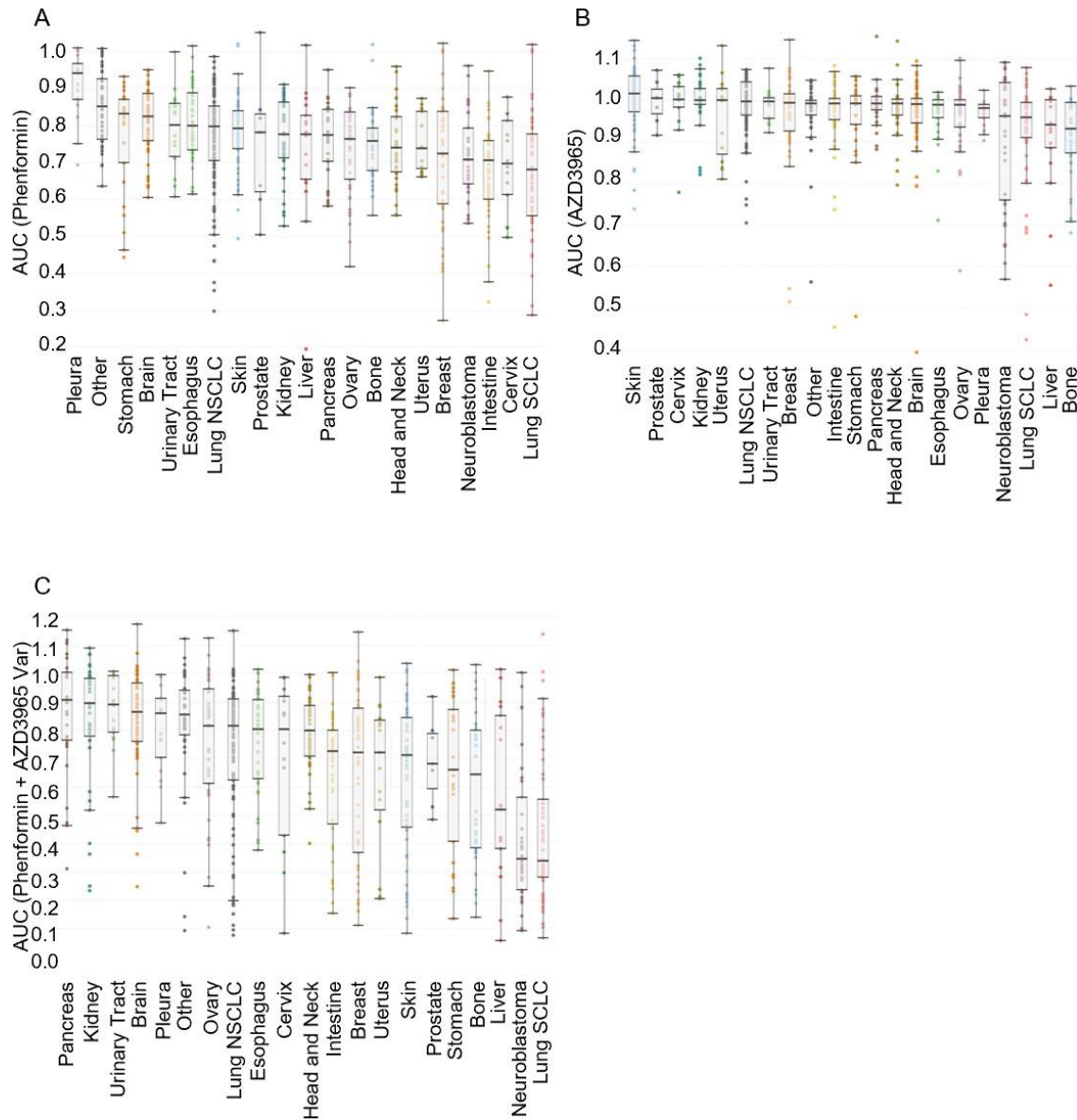
Metabolomic Analysis. Individual samples were subjected to methanol extraction then split into aliquots for analysis by ultrahigh performance liquid chromatography/mass spectrometry (UHPLC/MS). The global biochemical profiling analysis comprised of four unique arms consisting of reverse phase chromatography positive ionization methods optimized for hydrophilic compounds (LC/MS Pos Polar) and hydrophobic compounds (LC/MS Neg), as well as HILIC chromatography method coupled to negative (LC/MS Polar) (72). All methods alternated between full scan MS and data dependent MS scans. The scan range varied slightly between methods but generally covered 70-1000 m/z . Metabolites were identified by automated comparison of the ion features in the experimental samples to a reference library of chemical standard entries that included retention time, molecular weight (m/z), preferred adducts, and in-source fragments as well as associated MS spectra and curated by visual inspection for quality control using software developed at Metabolon. Identification of known chemicals entities was based on comparison to metabolomic library entries of purified standards (73).

qRT-PCR. The total RNA from cells was isolated with Quick-RNA Miniprep kit (Zymo Research). The complementary DNA was synthesized from 700 ng of total RNA by SuperScript III Reverse Transcriptase (Invitrogen) with Oligo(dT) primer (Ambion). The RT-qPCR analysis was performed in triplicate with SYBR Green master mix (Life Technologies) on a 7500 Fast Real-Time PCR system (Thermo Fisher Scientific) according to the manufacturer's protocol. The primer information is as follows: β -actin (F) 5'-GGCATGGGTCAGAAGGATT-3', (R) 5'-AGGATGCCTCTCTTGCTCTG-3', MCT1 (F) 5'-TGTTGTTGCAAATGGAGTGT-3', (R) 5'-AAGTCGATAATTGATGCCCATGCCAA-3', COX1 (F) 5'-ATTTAGCTGACTCGCCACACTCC-3', (R) 5'-ATACAATGCCAGTCAGGCCACC-3', COX2 (F) 5'-ACAGATGCAATTCCCGGACGTC-3', (R) 5'-TGGGCATGAACTGTGGTTTGCTC-3', ND1 (F) 5'-TGCGAGCAGTAGCCAAACAAT-3', (R) 5'-TGATGGCAGGATAATCAGAGG-3', MCT4 (F) 5'-TGCCATTGGTCTCGTGCTG-3', (R) 5'-TCTGCCTTCAGGAAGTGCTCC-3'.

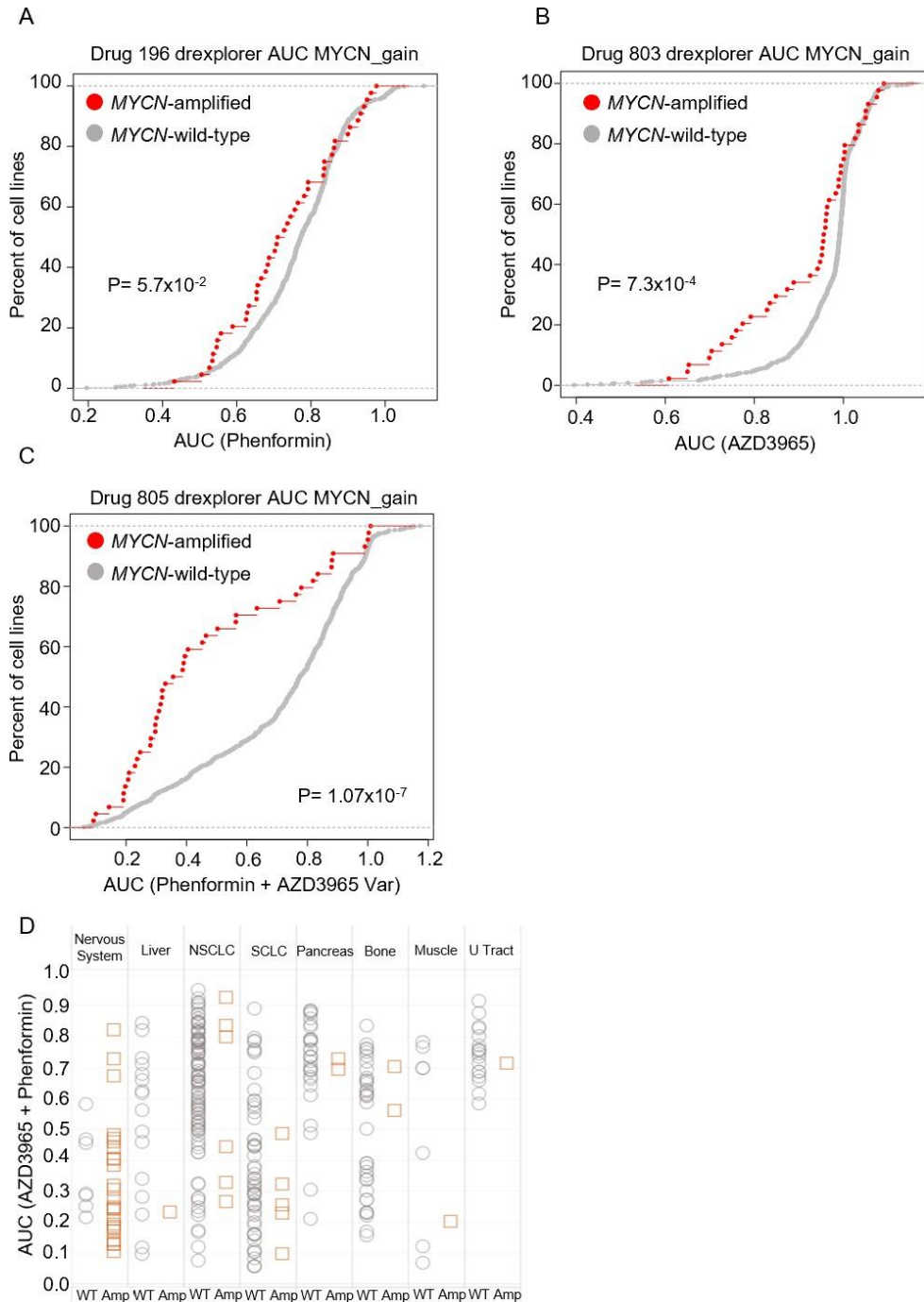
Statistical analyses. The datasets are indicated in the manuscript and figure legends. For the SEQC dataset, the "custom" analysis was used for Fig. 5C and the "RPM" analysis for rest of the SEQC panels. For statistical analyses biological triplicates were used unless otherwise stated. Statistical analyses were performed using a Kolmogorov-Smirnov two sample test for Fig. 1B and *SI Appendix*, Fig S2 A-C. Statistical analyses were performed using Welch's T-test for Fig. 1 D and E and *SI Appendix* Fig. S5. Statistical analyses were performed using the Mann-Whitney *U* test for Fig. 4A, with a Benjamini-Hochberg adjustment for *P*-values. Statistical analyses were performed using the Mann-Whitney *U* test for Fig. 5D, and Fig. 8C. Pearson's correlation coefficient and Student's t-test were used for Fig. 5F and 7F, and Student's t-test were used for Fig. 4 B and C, 6 A-C and F, and 8B, and for *SI Appendix*, Fig. S3 B, C, E and F, S7A, and S8 A and B. All other statistical analyses were performed using ANOVA and considered statistically different if $P < 0.05$.

Supplemental References

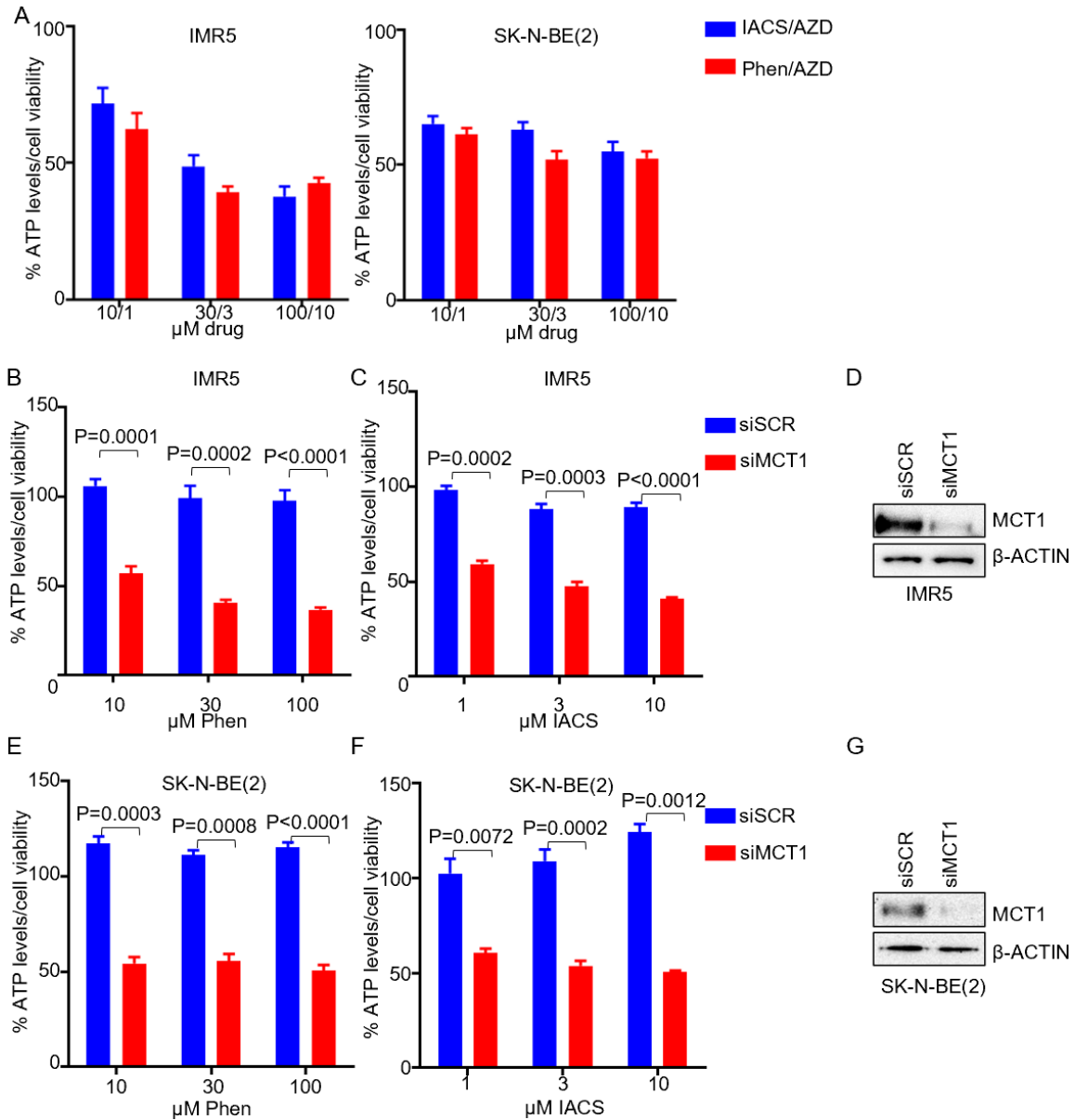
70. M. Nakagawa, N. Takizawa, M. Narita, T. Ichisaka, S. Yamanaka, Promotion of direct reprogramming by transformation-deficient Myc. *Proc. Natl. Acad. Sci. U.S.A.* 107, 14152–14157 (2010).
71. A. C. Faber et al., Differential induction of apoptosis in HER2 and EGFR addicted cancers following PI3K inhibition. *Proc. Natl. Acad. Sci. U.S.A.* 106, 19503–19508 (2009).
72. E. A.M. et al., High resolution mass spectrometry improves data quantity and quality as compared to unit mass resolution mass spectrometry in high-throughput profiling metabolomics. *Metabolomics* 4 (2014).
73. C. D. DeHaven, A. M. Evans, H. Dai, K. A. Lawton, Organization of GC/MS and LC/MS metabolics data into chemical libraries. *J. Cheminform* 2, 9 (2010).



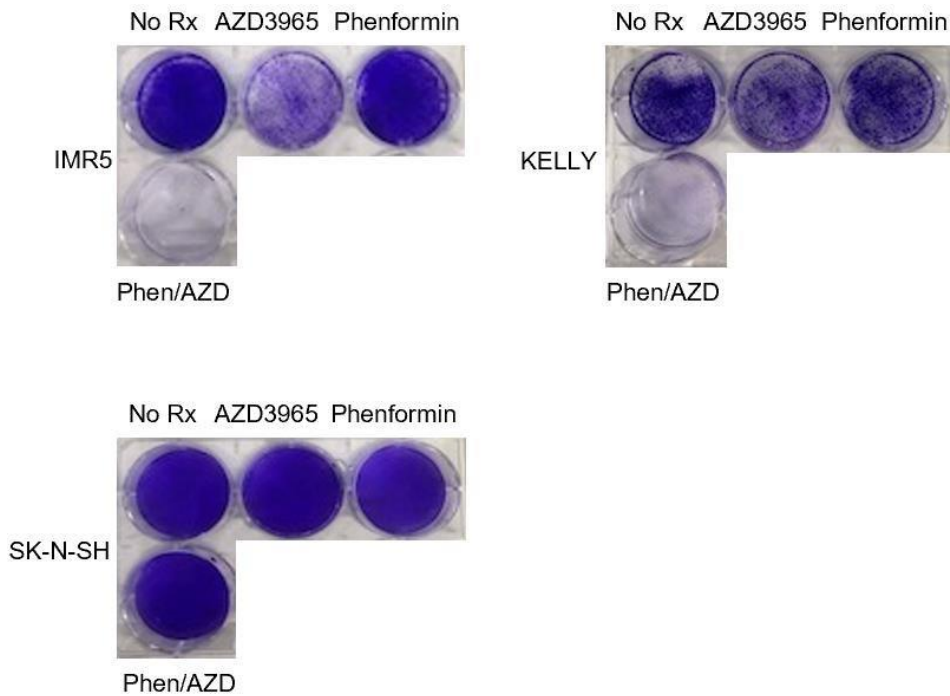
Sup. Fig. 1: The high-throughput screening reveals sensitivity of the AZD3965/phenformin combination in neuroblastoma. The distribution of sensitivity across cancer types for treatment with (A) phenformin alone, (B) AZD3965 alone, or (C) the combination of a fixed dose of phenformin (125 μ M) and variable dose of AZD3965 (256 nM – 1 nM). The area under the dose response curve (AUC) is used as the sensitivity measurement.



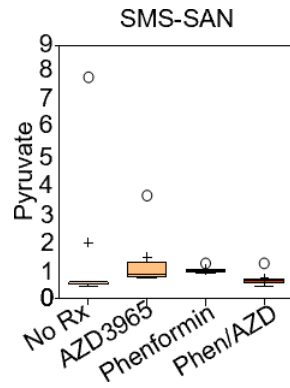
Sup. Fig. 2: The screen shows sensitivity of *MYCN*-amplified neuroblastoma to AZD3965/phenformin. The differential cumulative distribution of AUC values for *MYCN*-amplified versus *MYCN* wild-type cell lines treated with (A) phenformin alone, (B) AZD3965 alone, (C) the combination of fixed phenformin and variable AZD3965. The AUC values (X axis) are plotted against the percent of cell lines for each genotype (red: *MYCN*-amplified, gray: *MYCN* wild-type). The *P*-values were computed using a KS test. (D) The distribution of AUC values in cell lines groups bearing *MYCN*-amplification divided according to tissue of origin and *MYCN*-amplification status (*MYCN* wild-type in gray and *MYCN*-amplified in red).



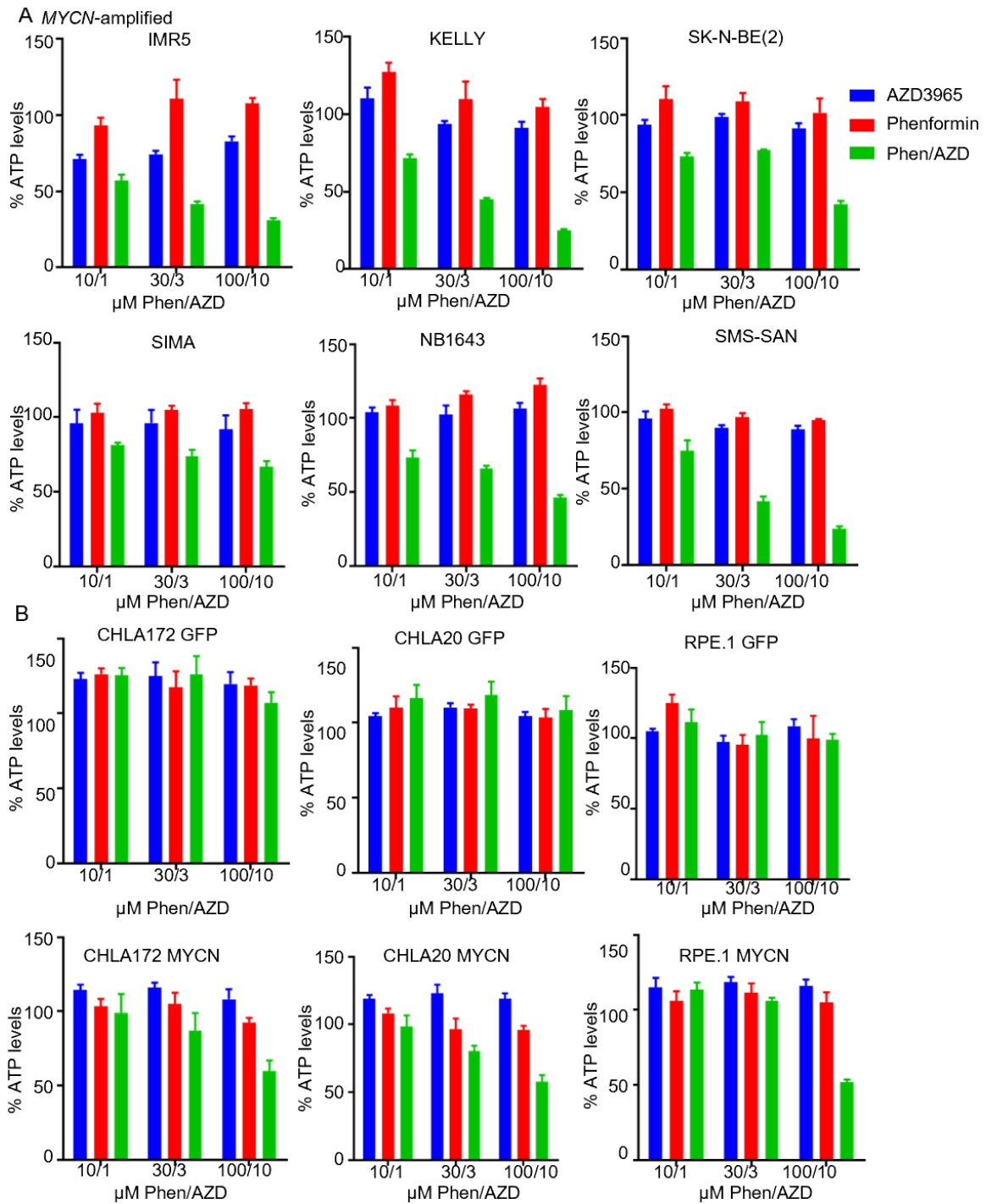
Sup. Fig. 3: (A) ATP/viability assays (CellTiter-Glo) were performed for the IMR5 and SK-N-BE(2) cells treated with AZD3965 (1, 3, or 10 μM), in combination with either phenformin (10, 30, or 100 μM), or IACS-010759 (1, 3, or 10 μM), at the indicated concentrations. ATP/viability assays (CellTiter-Glo) were performed in the IMR5 cells reverse transfected with small interfering (si) scramble or MCT1 siRNA and treated with (B) phenformin (10, 30, or 100 μM) or (C) IACS-010759 (1, 3, or 10 μM) at indicated concentrations. (D) Western blot of the IMR5 cells reverse transfected with small interfering (si) scramble or MCT1 siRNA and probed with the indicated antibodies. ATP/viability assay (CellTiter-Glo) were performed in the SK-N-BE(2) cells reverse transfected with si scramble or MCT1 siRNA and treated with (E) phenformin (10, 30, or 100 μM) or (F) IACS-010759 (1, 3, or 10 μM) at the indicated concentrations. (G) Western blot of the SK-N-BE(2) cells reverse transfected with si scramble or MCT1 siRNA and probed with the indicated antibodies.



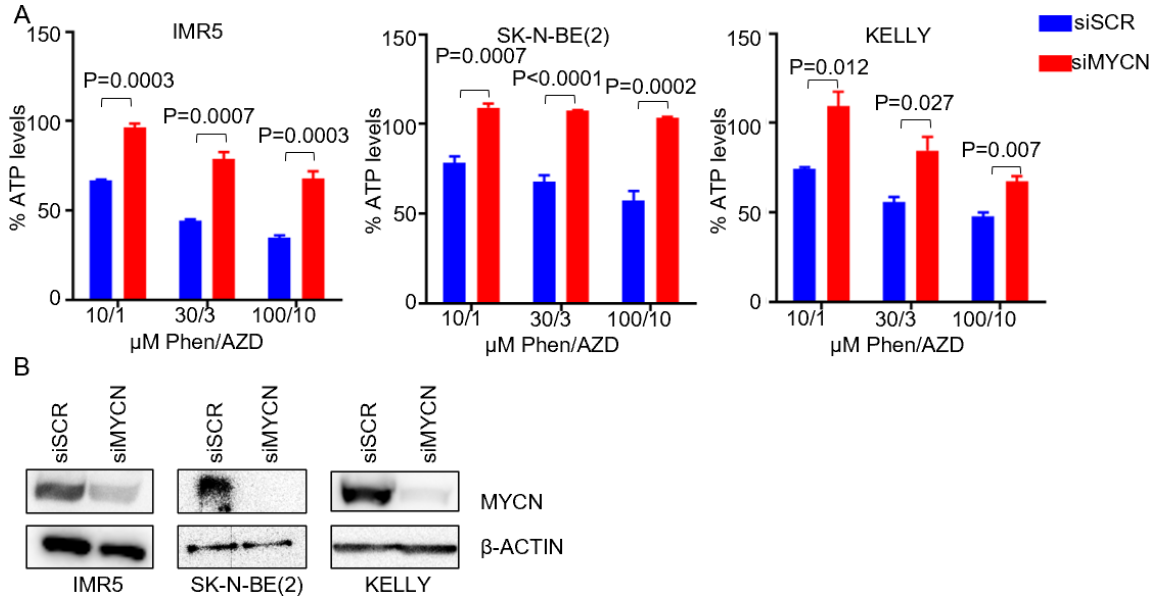
Sup. Fig. 4: The choice of media has no effect on combination sensitivity. Crystal violet assays of the indicated NB cell lines treated with 1 μ M AZD3965, 10 μ M phenformin, or the combination of both. The *MYCN*-amplified cell line IMR5 was cultured in RPMI (contains no pyruvate), the *MYCN*-amplified cell line KELLY was cultured in DMEM:F12 (contains pyruvate) and the *MYCN* wild-type cell line SK-N-SH was cultured in RPMI.



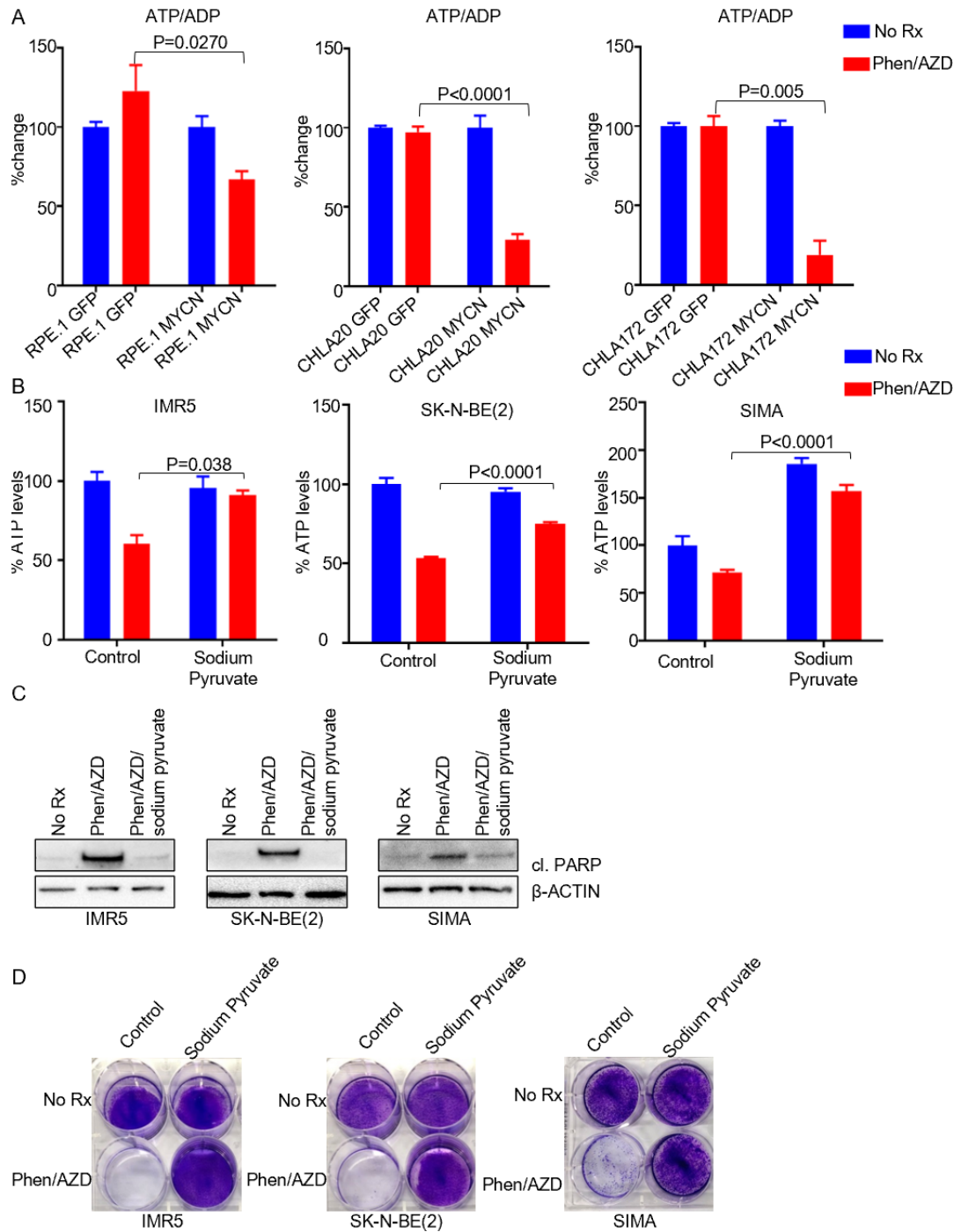
Sup. Fig. 5: The combination of AZD3965/phenformin has no effect on levels of pyruvate. Lysates of SMS-SAN cells following treatment with no drug (No Rx), 1 μ M AZD3965, 10 μ M phenformin, or the combination of both (n=5 for all groups) for 48 h underwent metabolic analysis through mass spectroscopy to measure the expression of pyruvate.



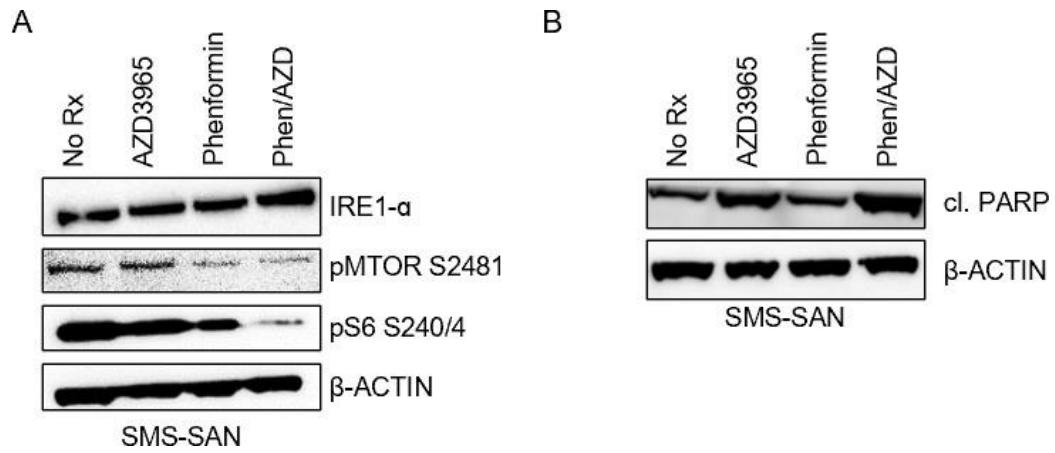
Sup. Fig.6: AZD3965/phenformin synergizes in *MYCN*-amplified neuroblastoma at an early time-point (16 h). ATP/viability assay (CellTiter-Glo) were performed in (A) *MYCN*-amplified cell lines and (B) syngeneic cell line pairs expressing exogenous *MYCN* or exogenous GFP as a control after 16 h treatment of AZD3965 (1, 3, or 10 μM), phenformin (10, 30, or 100 μM), or the combination of both at the indicated concentrations.



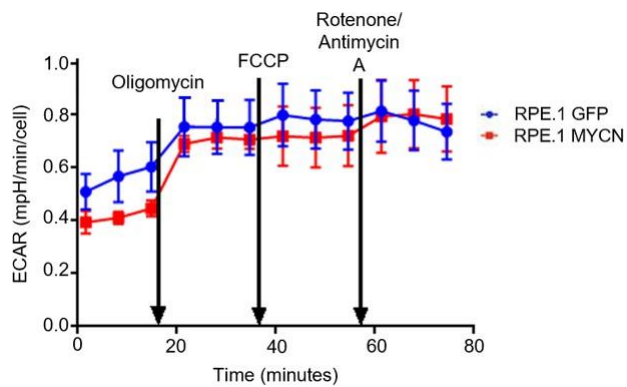
Sup. Fig. 7: Silencing of MYCN leads to protection from the combination therapy. (A) ATP/viability assay (CellTiter-Glo) were performed in *MYCN*-amplified cell lines reverse transfected with small interfering (si) scramble or MYCN si-RNA after 16 h treatment of AZD3965 (1, 3, or 10 µM), phenformin (10, 30, or 100 µM), or the combination of both at the indicated concentrations. (B) Western blot of cells reverse transfected with si-scramble or MYCN si-RNA probed with the indicated antibodies.



Sup. Fig. 8: Sensitivity to AZD3965 and phenformin causatively linked to *MYCN* amplification status. (A) Percent change in the ATP/ADP ratio in syngeneic cell line pairs expressing exogenous *MYCN* or exogenous GFP after 16 h treatment of 1 μ M AZD3965, 10 μ M phenformin, or the combination of both. (B) ATP/viability assay (CellTiter-Glo) were performed in *MYCN*-amplified cell lines treated with 1 μ M AZD3965 and 10 μ M phenformin for 16 h with or without the addition of 10mM sodium pyruvate. (C) Western blot of *MYCN*-amplified cell lines treated with 1 μ M AZD3965, 10 μ M phenformin with or without the addition of 10 μ M sodium pyruvate for 24 h probed with the indicated antibodies. (D) Crystal violet assay following 5 to 7 d of treatment with 1 μ M AZD3965, 10 μ M phenformin, with or without the addition of 10 mM sodium pyruvate in *MYCN*-amplified cell lines.



Sup. Fig. 9: AZD3965/phenformin induces cell death in *MYCN*-amplified neuroblastoma. (A, B) Western blot of SMS-SAN cells treated with 1 μ M AZD3965, 10 μ M phenformin, or the combination of both for 48 h probed with indicated antibodies.



Sup. Fig. 10: The expression of exogenous MYCN does not affect ECAR. RPE.1 GFP and MYCN expressing cells were analyzed with the Seahorse XFp mitochondrial stress test to measure ECAR.

Sup. Table 1: Compounds utilized in high-throughput screening with primary target and maximum concentration listed from 2-fold serial dilutions.

Compound #	Drug Name	Primary Target	High μM
196	Phenformin	Complex I	2000
803	AZD3965	MCT1	0.256
804	AZD3965 (0.128 μM fixed) + Phenformin var	MCT1 + Complex I	2000
805	Phenformin (125 μM fixed) + AZD3965 var	MCT1 + Complex I	0.256

Dataset S1: AUC values from HTS. Area under the curve values determined using drexplorer R package for cell lines from multiple tissues of origin treated with variable concentrations of AZD3965 and phenformin across 9 doses using 2-fold serial dilutions for 5 d.

Dataset S2: Viability values from GDSC. Resazurin was used to determine viability of cell lines of different tissues of origin treated with AZD3965 and phenformin across 9 doses using 2-fold serial dilutions for 5 d.

Dataset S3: Metabolite analyses of the SMS-SAN cells. Global biochemical profiling analysis was performed through ultra-high performance liquid chromatography/mass spectrometry.

Dataset S4: Elastic net regression. Output of the elastic net regression modeling of the AUC data to determine changes in gene expression from AZD3965, phenformin, the combination of fixed AZD3965 + variable phenformin, and the combination of fixed phenformin and variable AZD3965. Gene expression associated with a positive effect value corresponds to genes with high expression in the more resistant cell lines (high AUC values associated with high gene expression values).

Dataset S5: Relative gene expression for cells lines of various tissues of origin. Gene expression from elastic net regression in multiple cell lines from the GDSC treated with the combination of AZD3965 and phenformin.